

# Quantization of binding energy of structural solitons in passive mode-locked fiber lasers

Andrey Komarov,<sup>1,2</sup> Konstantin Komarov,<sup>2</sup> and François Sanchez<sup>1</sup>

<sup>1</sup>Laboratoire POMA, FRE CNRS 2988, Université d'Angers, 2 Boulevard Lavoisier, 49000 Angers, France

<sup>2</sup>Institute of Automation and Electrometry, Russian Academy of Sciences, Acad. Koptyug Pr. 1, 630090 Novosibirsk, Russia

(Received 14 January 2009; published 6 March 2009)

On basis of numerical simulation of fiber laser passive mode locking, we have determined the quantum binding-energy levels for a pair of interacting structural solitons. These solitons have powerful wings and correspondingly large binding energies. It has been found that the field amplitude functions for steady states corresponding to neighboring energy levels have opposite parity. We have pointed out the analogy between the energy quantization for laser bound solitons and for a particle moving in potential well. The possibility of a coexistence of in-, opposite-, and  $\pi/2$ -phase soliton pairs has been found. In the case of multiple soliton trains, we have demonstrated the realization of highly stable soliton sequences with any required distribution along the soliton train of various types of bonds between neighboring pulses.

DOI: 10.1103/PhysRevA.79.033807

PACS number(s): 42.65.Tg, 42.60.Fc, 42.65.Sf

## I. INTRODUCTION

Stable self-localized waves called solitons arise spontaneously in many fields of physics, among them hydrodynamics, plasma physics, superfluidity, nonlinear optics, and so on [1–3]. The passive mode-locked fiber lasers are of great interest for a study of various soliton properties in dissipative systems. Nonlinear-dispersion parameters of the fiber laser can be changed in a very large range that provides a distinct manifestation of these properties including diverse peculiarities of an interaction between solitons. The multiple-pulse passive mode locking is a commonly observed regime of operation for fiber lasers exploiting nonlinear polarization rotation technique [4–6]. As this takes place, the ultrashort pulses in a laser cavity have the same spectral and spatial parameters that caused by the effect of quantization of intracavity radiation into identical individual solitons [6,7]. The interaction between solitons plays a crucial role in the established multiple-pulse lasing regime. In the case of pulse attraction, the regime of bound solitons can be realized [8]. If this attraction is sufficiently strong, the soliton sequences become long. The quantity of solitons in the train can be equal to several hundreds [9]. Under certain conditions the harmonic bound-soliton passive mode-locking can be realized [10]. In this case the solitons are equidistantly placed in the laser cavity. The interaction between solitons is one of the main problems in the creation of soliton-based optical fiber communications lines. Such interaction can destroy or protect information sequences of ultrashort pulses. Thus, for efficient control and management of multiple soliton regimes it is necessary to know the properties of soliton interaction at a fundamental level.

Bound states of two solitons in the frame of complex cubic-quintic Ginzburg-Landau equation were first analyzed by Malomed [11]. Using standard perturbation analysis for soliton interaction, it was found solutions in the form of bound states of two solitons, which are either in-phase (the phase difference in the points of peak intensity of solitons is equal to zero) or opposite-phase (the phase difference is equal to  $\pi$ ). However, the detailed analysis showed that these types of bound states are unstable for used nonlinear-

dispersion parameters [12,13]. In the frame of this equation, Akhmediev *et al.* [8] discovered stable solutions which describe bound states of two solitons with a  $\pi/2$  phase difference between them. The bound states of solitons were then experimentally observed in passive mode-locked fiber lasers with the nonlinear polarization rotation technique [14–20]. The bound steady states with the  $\pi/2$  phase difference were detected in the experiments presented in the papers [15,20]. The authors of the paper [14] reported the observation of bound steady states with the  $\pi$  phase difference. In their experiment no bound states with a zero phase difference have been observed. The stable soliton pairs with zero and  $\pi$  phase differences were obtained on basis of the coupled extended Schrödinger equations that explicitly take into account the birefringence of the fiber and the gain and loss of the laser cavity [21,22]. In above investigations, both theoretical and experimental results were however limited to a few pulses.

The reliable experimental realization of long trains of bound solitons (several hundreds pulses in the train) [9] means their high stability that is caused by high binding energies of solitons. Recently we have found the type of solitons which we named “structural solitons” [23]. These solitons have powerful wings that result in large binding energies of interacting pulses. This paper is devoted to a theoretical investigation of bound steady states of structural solitons. For our numerical analysis we used the model which describes adequately a dependence of nonlinear losses on a field intensity for real fiber lasers with the nonlinear polarization rotation technique in all range of laser parameters [6]. For some conditions this model transforms into one which is determined by the complex cubic-quintic Ginzburg-Landau equation [24].

This paper is organized as follows. In Sec. II we present the used model of a passive mode-locked fiber laser with nonlinear polarization rotation technique and the corresponding equations describing the soliton dynamics. Section III is devoted to the numerical simulation results on the quantization of a binding energy of a soliton pair with zero and  $\pi$  phase difference, on the information bound-soliton sequences, and on the coexistence of soliton pairs with different phase differences including the  $\pi/2$  phase difference be-

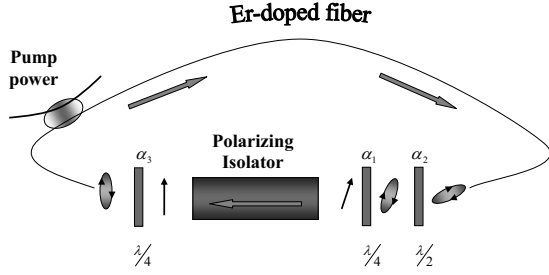


FIG. 1. Schematic representation of the investigated fiber ring laser passively mode locked through nonlinear polarization rotation.

tween solitons. In Sec. IV we give the physical interpretation of the energy quantization based on boundary conditions for two waves describing individual solitons. Section V is devoted to the discussion of the obtained results.

## II. PHYSICAL MODEL AND MASTER EQUATIONS

The laser under investigation is schematically represented in Fig. 1. It was described in detail in Ref. [6]. For isotropic fiber, this system involves all necessary elements for the control of nonlinear losses. After the polarizing isolator the electric field has a well-defined linear polarization. Such state of polarization does not experience polarization rotation in the fiber because the rotation angle is proportional to the area of the polarization ellipse. Consequently, it is necessary to place a quarter-wave plate 3 which transforms the linear polarization into the elliptic one ( $\alpha_3$  represents the orientation angle of one eigenaxis of the plate with respect to the laboratory frame). The rotation of the polarization ellipse resulting from the optical Kerr nonlinearity is proportional to the light intensity, the area of the polarization ellipse and the fiber length. At the output of the fiber, the direction of the elliptical polarization of the central part of the pulse can be rotated toward the passing axis of the polarizer by the half wave plate 2 (the orientation angle is  $\alpha_2$ ). Then this elliptical polarization can be transformed into a linear one by the quarter-wave plate 1 (the orientation angle is  $\alpha_1$ ). In this situation the losses for the central part of the pulse are minimized while the wings undergo strong losses. The evolution of the radiation in the investigated laser is described by the following set of equations [6]:

$$\frac{\partial E}{\partial \zeta} = (D_r + iD_i) \frac{\partial^2 E}{\partial \tau^2} + (G + iq|E|^2)E, \quad (1)$$

$$E_{n+1}(\tau) = -\eta[\cos(pI_n + \alpha_0)\cos(\alpha_1 - \alpha_3) + i \sin(pI_n + \alpha_0)\sin(\alpha_1 + \alpha_3)]E_n(\tau), \quad (2)$$

where  $E(\zeta, \tau)$  is the electric field amplitude,  $\tau$  is a time coordinate expressed in units  $\delta t = \sqrt{|\beta_2|}L/2$  (here  $\beta_2$  is the second-order group-velocity dispersion for fiber and  $L$  is the fiber length),  $\zeta$  is the normalized propagation distance  $\zeta = z/L$ ,  $D_r$  and  $D_i$  are the frequency dispersions for a gain loss and for a refractive index, respectively, and  $q$  is the Kerr nonlinearity. The term  $G = a/(1 + b\int|E|^2 d\tau)$  in the second parenthesis in Eq. (1) describes the saturable amplification

(here the integration is carried out on the whole round-trip period,  $a$  is the pumping parameter and  $b$  is the saturation one). The second term in these parentheses is connected with Kerr nonlinearity of the fiber. Equation (2) determines the relation between the time distributions of the field before and after  $n$ th pass of radiation through the polarizer ( $\eta$  is the transmission coefficient of the intracavity polarizer). Parameters  $\alpha_0$ ,  $I$ , and  $p$  are determined by relations  $\alpha_0 = 2\alpha_2 - \alpha_1 - \alpha_3$ ,  $I = |E|^2$ ,  $p = \sin(2\alpha_3)/3$ . The amplitude  $E(\tau)$  is subject to periodic boundary conditions with period equal to one round trip.

The numerical procedure starts from the evaluation of the electric field after passing through the Kerr medium, the phase plates, and the polarizer, using Eq. (2). The resulting electric field is then used as the input field to solve Eq. (1) over a distance  $L$ , using a standard split-step Fourier algorithm. The computed output field is used as the new input for Eq. (2). This iterative procedure is repeated until a steady state is achieved.

## III. RESULTS OF NUMERICAL SIMULATION

### A. Steady states of two bound solitons

For our numerical simulation we have used typical parameters of Er-doped fiber laser with anomalous net dispersion of group velocity. Figure 2 shows the temporal and spectral profiles of a single soliton. The soliton has significant wings. On the bell-shaped spectral profile one can see the additional structure. For some nonlinear-dispersion parameters of an intracavity medium, the additional structure arises also on powerful wings of the temporal intensity profile of a pulse. This structure can depend on initial generation conditions. In paper [23] such solitons have been named structural solitons. The sidebands in the soliton spectrum are typical for case of anomalous dispersion. In the frame of the model described by Eqs. (1) and (2), the top part of the soliton and its pedestal are formed by different mechanisms. The former is mainly shaped by the combined action of the focusing nonlinearity and the anomalous dispersion of refractive index. The latter is formed also by the nonlinear losses. As a result, choosing suitable angles of the phase plates  $\alpha_i$  and dispersion parameters ( $D_r$ ,  $D_i$ ), we can independently change properties of the pedestal and the top part of a soliton in wide limits. By this method we have obtained the regime in which stable solitons and stable cw-component of radiation coexist simultaneously [25].

Because of the interaction between solitons, the pair of such structural solitons is united in the stability formation with a large binding energy—highly stable “two-soliton molecule” [8]. The radiation energy of such molecule is less than the energy of two solitons placed from each other on a long distance. The binding energy for two solitons in this molecule takes the discrete set of values shown in Fig. 3. Corresponding energy levels are numbered in decreasing order for a binding energy presented in relative units (the binding energy divided by twice the energy of an isolated soliton). The binding energy is the difference between the energy of the bound-soliton pair and two widely separated identical solitons. Large binding energies for the low-energy steady states

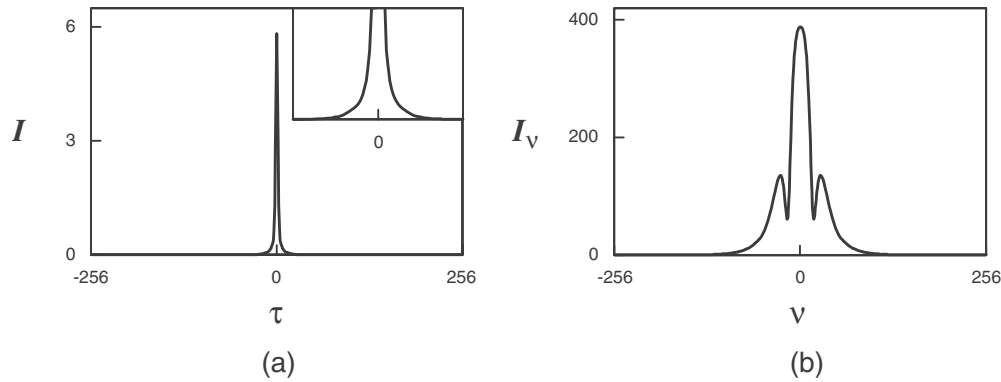


FIG. 2. (a) Temporal and (b) spectral distributions of radiation for the single soliton passive mode locking. The upper right inset of Fig. 2(a) shows the multiplied soliton pedestal. In all figures we use arbitrary units.  $a=1.1$ ,  $q=2$ ,  $D_i=0.13$ ,  $\alpha_0=0.2$ ,  $\alpha_1=-1.64$ ,  $\alpha_3=0.2$ ,  $D_r$  is determined by the amplification medium:  $D_r=D_{r0}G$ ,  $D_{r0}=0.085$ .

are due to powerful wings of the structural solitons.

For the ground steady state (the first energy level) and for the all odd levels, the field functions are antisymmetric  $E_k(\tau)=-E_k(-\tau)$  if the origin of the coordinate  $\tau=0$  corresponds to the point equally spaced from the peaks of the solitons. In this case, the peaks amplitudes of two solitons are in opposite phase ( $\delta\varphi=\pi$ ). For all even steady states the field functions are symmetric  $E_k(\tau)=E_k(-\tau)$  and the peaks amplitudes of two solitons have the same phase ( $\delta\varphi=0$ ).

In the ground state the distance between the solitons is minimal  $d_1$ . For the  $k$ th steady state this distance  $d_k$  is determined by the approximate relation

$$d_k \approx kd_1. \tag{3}$$

In our numerical experiment the second soliton is placed in the points in which the phase of the single first soliton is multiple  $\pi$  (the phase of the single first pulse in the point of its peak intensity is supposed equal to zero). The distances between these points and the point of a peak intensity of the first single pulse are correspondingly also determined by Eq. (3). For the laser parameters we used, the phase of a single soliton in the vicinity of its central part changes nonmonotonically. As a result, the phases in the first point  $d_1$  and in the point of a peak intensity are the same. For the first steady state with the distance between solitons  $d_1$  (the ground

steady state) the phase difference for their amplitudes in their peak points is  $\pi$ . This means the opposite-phase interference between the central part of each of two pulses with a wing of other one in the case of ground steady state. On basis of the presented numerical simulation results it is easy to understand that this statement is true for any obtained steady state. Thus, the results of our numerical simulation show the opposite-phase (destructive) interference between the central part of each of two pulses with a wing of other one for all discussed here steady states.

All steady states are stable. This means multistability of such two-soliton molecule. Setting some distance between initial pulses, after a transient process we have obtained the steady state, for which the distance between pulses is the closest to its initial distance. This result depends weakly on an initial phase difference. During transient process the phase difference corresponding to a realized steady state is established very quickly (about ten round-trip periods).

Figure 4 shows the temporal distributions of intensities in the two-soliton molecule for the cases of the ground steady state (the minimal distance between solitons) and for the first and second excited steady states (the distances between solitons approximately equals the double and triple minimal one  $d_1$ , respectively). In the cases of the ground ( $k=1$ ) and second excited ( $k=3$ ) states, the intensity is equal to zero in the center point between solitons. For the first-excited state  $k=2$  the intensity in this point is distinct from zero.

Our numerical simulation shows that the soliton pairs in different steady states can coexist each with other and with single solitons. Note that similar results on quantization of soliton separation in a soliton pair have been previously reported in a different configuration [26]. Indeed, it was considered a stretched pulse fiber laser and the resulting separation did not vary in arithmetic progression.

### B. Information sequences of bound solitons

Due to large binding energies, it is possible to realize highly stable noise-proof multisoliton molecules. Placing several initial pulses on certain distances from each other, after transient process we have obtained stationary “molecular chains” with any desirable distribution of types of bonds

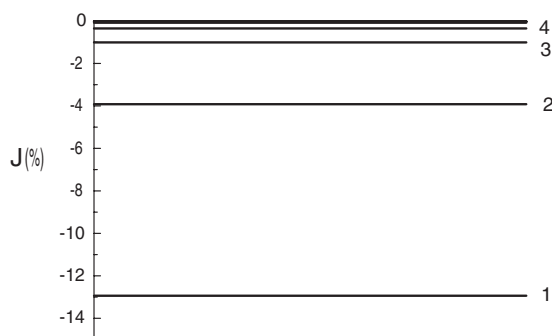


FIG. 3. Binding energy of two solitons in steady states  $J$  expressed in relative units (the binding energy divided by the energy of the two solitons removed from each other on the long distance). The laser parameters are the same as in the case of Fig. 2.

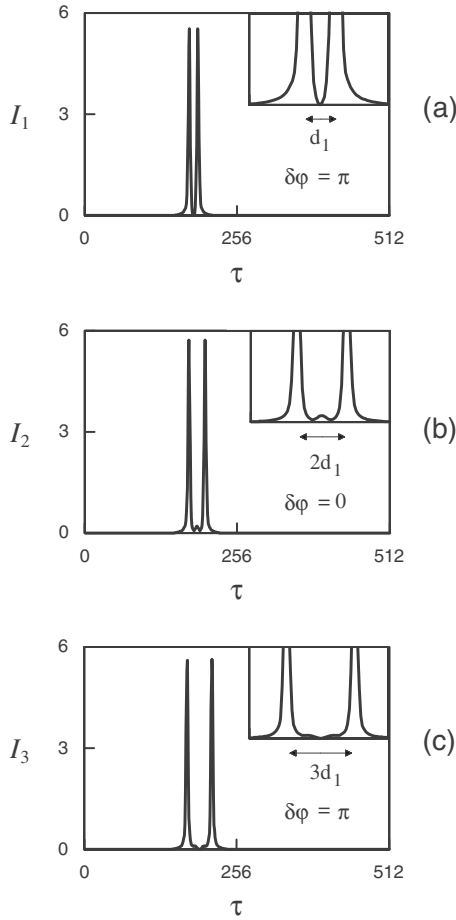


FIG. 4. Temporal distribution of intensity in the two-soliton molecule for (a) the ground steady state (minimal distance  $d_1$  between solitons), for (b) the first-excited steady state, and for (c) the second excited steady state. The laser parameters are the same as in the case of Fig. 2.

between neighboring solitons along a pulse train. Such sequence is realized more simply with a use of the ground- and first-excited types of intersoliton bonds for which the binding energies are especially great. Distributing types of intersoliton bonds along a soliton train by required appointed order, it is possible to code information. Figure 5 shows such information soliton sequence in which the number 2708 is coded in binary system. Here the ground type of a bond (smaller distance between pulses) corresponds to zero and the first-excited type of a bond (the greater distance between pulses) corresponds to unit. In binary system this sequence corresponds to the number 101010010100, that in decimal system is the number 2708.

Such soliton trains are highly stable formations. The high stability is primarily due to large binding energies. Furthermore, there exists a second reason of the high stability. It consists in the following. The perturbation energy which was initially localized in the vicinity of some pair of bound solitons is quickly collectivized among all solitons of the train. In the numerical simulation we have used the random radiation noise to prove this stability. This noise induces up to 10% fluctuations of peak intensities of solitons but does not change the structure of soliton sequences.

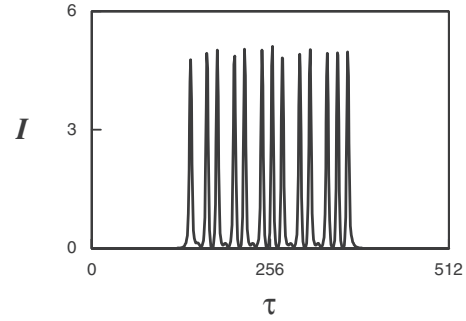


FIG. 5. Stable train of bound solitons with the ground- and first-excited types of bonds in which the number 2708 is coded in binary system 101010010100. The greater distance between pulses corresponds to unit. The smaller distance between pulses does to zero. The laser parameters are the same as in the case of Fig. 2.

**C. Nonsymmetric steady states of a bound-soliton pair**

The phase difference for solitons in the above-discussed symmetric and antisymmetric pairs is equal to zero and  $\pi$ , respectively. Such soliton pairs and also soliton trains with symmetric and antisymmetric types of bonds (see Fig. 5) move at the same velocity as single solitons. In our numerical experiment we have also observed bound states of two solitons with a phase difference  $\pi/2$  [8,26]. These nonsymmetric pairs of bound solitons move relative to single solitons, symmetric and antisymmetric soliton pairs, and relative to the above-mentioned soliton trains. Figure 6 demonstrates such movement and the elastic collision of a  $\pi/2$  soliton pair and a single soliton. After the collision the initially at-rest soliton and the forward soliton of the moving pair forms the new  $\pi/2$  pair which continues the movement. The tail soliton of the initial pair therewith transits in a state at rest. With other laser parameters we have observed a nonelastic collision of a nonsymmetric pair and a single soliton. In this case after the collision the stable moving structure with the three bound soliton were realized. These results are in excellent agreement with those obtained on basis of the complex cubic-quintic Ginzburg-Landau equation [27].

In our numerical experiment we have obtained regimes in which the  $\pi/2$  soliton pairs simultaneously coexist with

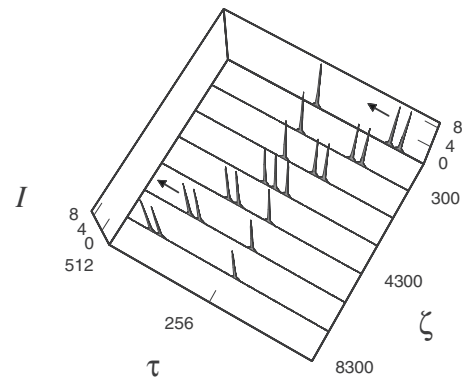


FIG. 6. Elastic collision between a soliton pair with a  $\pi/2$  phase difference and a single soliton.  $a=1.3$ ,  $\alpha_0=-0.1$ ,  $\alpha_3=0.17$ , the other parameters are the same as in the case of Fig. 2.



symmetric and antisymmetric pairs and with solitons sequences. With decreasing pumping the phase difference for the nonsymmetric soliton pair shown in Fig. 6 increases. When the pump reaches some threshold value, the nonsymmetric pair transforms into ground antisymmetric state. In the vicinity of the threshold of the transition the phase difference of the nonsymmetric pair is considerably different from  $\pi/2$ . With laser parameters for the case of Fig. 5 we could not obtain a  $\pi/2$  soliton pair. Nevertheless, the  $\pi/2$  bond was easily realized at the ends of soliton sequences with symmetric and antisymmetric bonds. As this takes place, the soliton sequence begins to move relative to single solitons.

#### IV. PHYSICAL INTERPRETATION OF BINDING-ENERGY QUANTIZATION

Physical interpretation of the obtained energy quantization consists in the following. Distances and phase relations for solitons in steady state take such values for which the arising field structure experiences minimal nonlinear losses. In the papers [6,7] we found that in the case of multiple-pulse passive mode locking the total amplification coefficient decreases with increasing peak intensity of a soliton. It is a necessary condition for an equalization of peak soliton amplitudes. Thus, the condition for minimal loss for a two-soliton structure is the opposite-phase interference of the central part of each of two pulses with a wing of other one. In this case the peak intensities of solitons are decreased and the amplification coefficients are correspondingly increased. The same interference is realized in our numerical experiment (see Sec. III A). In this way we obtain two boundary conditions which link the two-soliton waves to each other and result in a quantization of the energy binding the two solitons.

Let  $\varphi_1(\tau_{1\max})$  and  $\varphi_1(\tau_{2\max})$  be the phases of the field for the first soliton in points of its peak intensity and of the peak intensity of the second soliton, respectively. Similarly, we designate through  $\varphi_2(\tau_{2\max})$  and  $\varphi_2(\tau_{1\max})$  the phases of the amplitude for the second soliton in points of its peak intensity and of the peak intensity of the first soliton, respectively. The condition of an opposite-phase interference of two pulses in points of their maximal amplitudes can be written down as follows:

$$\varphi_1(\tau_{2\max}) = \varphi_2(\tau_{2\max}) - \pi + 2\pi k_1, \quad (4)$$

$$\varphi_2(\tau_{1\max}) = \varphi_1(\tau_{1\max}) - \pi + 2\pi k_2, \quad (5)$$

where  $k_1$  and  $k_2$  are integers. These relations are the two boundary conditions (in the points  $\tau = \tau_{1\max}$  and  $\tau = \tau_{2\max}$ ). Summarizing these two equalities, we obtain the following ratio:

$$\delta\varphi_1 + \delta\varphi_2 = 2\pi(k-1), \quad (6)$$

where  $\delta\varphi_1 = \varphi_1(\tau_{2\max}) - \varphi_1(\tau_{1\max})$  is the phase difference of the first soliton wave for the points  $\tau = \tau_{2\max}$  and  $\tau = \tau_{1\max}$ ,  $\delta\varphi_2 = \varphi_2(\tau_{1\max}) - \varphi_2(\tau_{2\max})$  is the phase difference of the second soliton wave for the points  $\tau = \tau_{1\max}$  and  $\tau = \tau_{2\max}$ ,

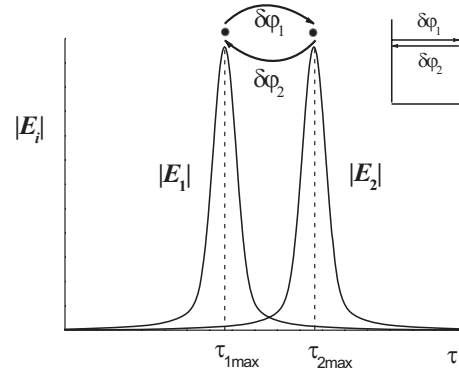


FIG. 7. Stationary steady states of “two-soliton molecule” corresponds to such distance between solitons for which the total change in a phase of a field on the closed trajectory  $\delta\varphi_1 + \delta\varphi_2$  is equal to  $2\pi(k-1)$ , where  $k$  is an integer. The closed trajectory consists of two parts: the first part from the point  $\tau_{1\max}$  up to the point  $\tau_{2\max}$  is related with a change in the phase for a wave function of the first pulse, and the second part from the point  $\tau_{2\max}$  up to the point  $\tau_{1\max}$  is related with a change in a phase for a wave function of the second pulse. The upper right inset gives the analogy with the mechanism of energy quantization for a particle moving in a square potential well with infinite walls.

$k = (k_1 + k_2)$  is an integer. Here  $k$  is determined by such way that it gives  $\delta\varphi_1 + \delta\varphi_2 = 0$  with  $k=1$  in the correspondence with our numerical results (see Sec. III A). Thus, from the two boundary conditions we have obtained the condition of the energy quantization and of the steady-state realization in the following form (see Fig. 7): the total change in the phase of a field on the closed trajectory is multiple  $2\pi$  (the closed trajectory consists in two parts: the first part from the point  $\tau_{1\max}$  up to the point  $\tau_{2\max}$  is related with a change in the phase for a wave function of the first pulse, and the second part from the point  $\tau_{2\max}$  up to the point  $\tau_{1\max}$  is related with a change in the phase for a wave function of the second pulse). As a matter of fact, this condition coincides with the condition of an energy quantization for a particle under its finite movement which is according to Bohr’s rule in the following formulation: on the closed trajectory of a movement of a particle, there should be an integer number of de Broglie’s wavelengths.

As characteristics of both pulses are identical (within a location on the axial period and any phase factor in the case of an absence of interference interactions), and the varying part of a phase for each pulse is even function of a variable  $\tau$ , then  $\delta\varphi_1 = \delta\varphi_2 = (k-1)\pi$ . It means that even  $k$  corresponds to symmetric distributions of a field in the soliton molecule  $E_k(\tau) = E_k(-\tau)$  (the solitons are in phase), and odd  $k$  does to antisymmetric distributions  $E_k(\tau) = -E_k(-\tau)$  (the solitons are in opposite phase). On wings of a pulse, the phase is monotonic function of  $\tau$ . Hence, with increasing  $k$ , the distance between pulses monotonously increases. With increasing  $k$ , the effect of redistribution of a field owing to an interference and an additional amplification due to such redistribution are decreased. It means that with increasing  $k$  the binding energy of a molecule is decreased. As pointed out above, the used here numbers  $k$  coincide with the numbers  $k$  of the energy levels shown in Fig. 3.

It is easy to understand why the distance between solitons in steady states is approximately multiple to the minimal distance. It is connected to the circumstance that local frequency of a field on wings of pulses practically does not vary [28], and the phase change along a pulse equal to  $\pi$  occurs after equal intervals  $\delta\tau$ . As a result, Eq. (3) is obtained.

It is necessary to note that, in the discussed task, an anti-symmetric wave function corresponds to the lowest binding-energy level, while from quantization of energy for a particle in a symmetric potential well, it is known that a wave function of the ground state is symmetric. Although in both cases the opposite-phase boundary conditions are used. In the case of a particle the minimum phase change between boundary points for each counterpropagating wave is  $\pi$ . In our case this is zero (the phase of a single soliton in the vicinity of its central part changes nonmonotonically). As a result, the ground states in these tasks have opposite parities. For other laser parameters for which the phase of a single soliton changes monotonously with changing  $\tau$  from the peak intensity point to infinity, one might expect that the ground steady state will be even.

In this paper we use the opposite-phase boundary conditions for a quantization of a binding energy of two interacting solitons. It is necessary to note that in the case of the in-phase boundary conditions the parity of each of steady state is replaced with the opposite parity. The distances between solitons are determined by Eq. (3) as for case of the opposite-phase boundary conditions. However these field configurations will not correspond to minimal losses and are not realized in an experiment.

In the case of only in-phase boundary conditions or only opposite-phase ones, steady states of a two-soliton molecule are described by symmetric or antisymmetric wave functions  $E_k(\tau)$ . The phase difference for solitons is zero or  $\pi$ . The energy flow between solitons is absent because of symmetry. If the energy flow for points 0 and  $\pi$  is equal to zero, it is naturally to expect that it will be maximal in an intermediate point where symmetry is maximally broken, which is in a vicinity of a point  $\pi/2$ . What boundary conditions are required for such phase difference? It is easy to understand that boundary conditions must be mixed ones: in the point of a peak amplitude of one soliton the interference must be constructive, in the point of a peak amplitude of other soliton it must be destructive. In this case, in the right part of one from Eqs. (4) and (5) there occurs the additional phase  $\pi$ . Equation (6) transforms into the equation  $\delta\varphi_1 + \delta\varphi_2 = 2\pi(k-1) + \pi$ . If the peak intensities of the solitons are almost the same then  $\delta\varphi_1 = \delta\varphi_2 = \pi/2 + \pi(k-1)$ . This means the  $\pi/2$  phase difference for bound solitons. The additional asymmetric chirp in the interior wings of the solitons due to the  $\pi/2$  phase difference results in a movement of the soliton pair relative to a single symmetric soliton. The energy balance in such molecule is realized in the following way. The energy flow goes from the smaller pulse to the greater one. As a result, they have the difference in their peak amplitudes which is due to this flow [29,30]. These energy changes in individual solitons are compensated by a difference in their amplification: the total amplification coefficient for the greater pulse is less than for a smaller one. The stability of a  $\pi/2$  bound pair means an energy advantage of such configura-

tion of the field. It would appear reasonable that the  $\pi/2$  bound pairs are the most easily realized if peak intensities of solitons correspond to the top part of dependence of the total amplification coefficient on a peak soliton intensity (see Fig. 9 in the paper [6] and Fig. 3 in the paper [7]). In this case the mechanism of equalization of solitons is the weakest.

So, the presented physical interpretation allows to identify the mechanism of quantization of the binding energy of a two-soliton molecule and to explain the basic laws of this quantization which have been revealed in the performed numerical experiment.

## V. DISCUSSION

The analysis on basis of complex cubic-quintic Ginzburg-Landau equation showed an instability of in- and opposite-phase steady states of a bound soliton pair and a stability of  $\pi/2$ -phase steady states [8,11–13]. For our analysis we used more generalized model taking into account peculiarities of intensity-dependent losses for real fiber lasers. In the frame of such model we have found stable steady states with all above-mentioned phase differences. We have shown that soliton pairs with in-, opposite-, and  $\pi/2$ -steady states can simultaneously coexist each with others and with single solitons. In our analysis we have not taken into account an anisotropy and a third-order dispersion of a fiber, because of these effects result in insignificant modifications of investigated phenomena.

In our study we have chosen such laser parameters for which the researched phenomena are manifested most clearly. With other parameters we have observed various modifications of investigated regimes. For examples, we have observed the temporal oscillations of soliton amplitudes in bound states. For some parameters the lower states were unstable. As a result of this instability, a soliton pair transits into a higher steady state. With other parameters this instability results in a merge of solitons. With certain parameters the investigated phenomena are masked by period-doubling effects.

Our results on  $\pi/2$  soliton pairs are in agreement with corresponding experimental and theoretical results obtained on basis the complex cubic-quintic Ginzburg-Landau equation [8,15,20,27]. It concerns character of collision of soliton pairs with single pulses. In our numerical simulation we have obtained the ground steady state with  $\pi$  phase difference for solitons in the pair. The binding energy for this ground state is considerably more than for the first-excited state (by factor 3). As a result, in an experiment the  $\pi$  bound steady state will be realized with the greater probability than in-phase states. Really, the transition of the pair from the ground steady state to excited states requires considerably greater energy than a return one. It may explain the experimental results of the paper [14] where a  $\pi$  bound state of a soliton pair was observed but the in-phase states were not detected. The authors of the papers [21,31,32] observed the lasing regime with several same pairs of bound solitons in the laser cavity. As this takes place, single solitons are always absent in the cavity. This fact can be understood if the binding energy of a soliton pair is greater than the energy of a single soliton. In

our numerical experiment it was 26% of the single soliton energy.

Thanks to large binding energies of interacting structural solitons, we have realized high-stable noise-proof multisoliton molecules. We have shown that sets of various types of bonds between neighboring pulses in such molecule can be obtained. Accordingly, the coding of the information in these soliton sequences can be realized through various distributions of types of bonds between neighboring pulses along a soliton train. Dense packing of pulses in the bound-soliton sequence provides high speed of transfer of information in fiber communications line working in nonlinear bound-soliton-based regime.

## VI. CONCLUSION

On basis of numerical simulation we have found that odd and even steady states of a soliton pair are determined by conditions of opposite-phase interference between a peak amplitude of each from two pulses and a wing of other pulse. The steady states corresponding to neighboring binding-energy levels have opposite parity. The ground steady state

has odd parity. All steady states are stable. From any initial state the soliton pair passes in one of possible steady states, that is, a bound-soliton pair is multistable. We have demonstrated the possibility to form information soliton sequences with any desirable distribution of the types of bonds between neighboring pulses along soliton trains. Thanks to large values of binding energies, such sequences have a high level of stability against perturbations.

We found that nonsymmetric steady states of two bound solitons with the  $\pi/2$  phase difference between them are determined by mixed boundary conditions: (1) the in-phase interference between a peak amplitude of first pulse and a wing of second pulse; (2) the opposite-phase interference between a peak amplitude of second pulse and a wing of first pulse. In-, opposite-, and  $\pi/2$ -phase soliton pairs can simultaneously coexist with each other and with single solitons.

## ACKNOWLEDGMENT

This research was supported by a Marie Curie program of the European Community Framework Programme (Grant No. 039942-PMLFL).

- 
- [1] N. N. Akhmediev and A. Ankiewicz, *Solitons* (Chapman and Hall, London, 1997).
  - [2] M. Remoissenet, *Waves Called Solitons* (Springer-Verlag, Berlin, 1994).
  - [3] I. S. Aranson and L. Kramer, *Rev. Mod. Phys.* **74**, 99 (2002).
  - [4] A. V. Grudinin, D. G. Richardson, and D. N. Payne, *Electron. Lett.* **28**, 67 (1992).
  - [5] D. Y. Tang, L. M. Zhao, B. Zhao, and A. Q. Liu, *Phys. Rev. A* **72**, 043816 (2005).
  - [6] A. Komarov, H. Leblond, and F. Sanchez, *Phys. Rev. A* **71**, 053809 (2005).
  - [7] A. K. Komarov and K. P. Komarov, *Phys. Rev. E* **62**, R7607 (2000).
  - [8] N. N. Akhmediev, A. Ankiewicz, and J. M. Soto-Crespo, *Phys. Rev. Lett.* **79**, 4047 (1997).
  - [9] A. Haboucha, H. Leblond, M. Salhi, A. Komarov, and F. Sanchez, *Phys. Rev. A* **78**, 043806 (2008).
  - [10] A. Komarov, A. Haboucha, and F. Sanchez, *Opt. Lett.* **33**, 2254 (2008).
  - [11] B. A. Malomed, *Phys. Rev. A* **44**, 6954 (1991).
  - [12] V. V. Afanasjev and N. Akhmediev, *Phys. Rev. E* **53**, 6471 (1996).
  - [13] V. V. Afanasjev, B. A. Malomed, and P. L. Chu, *Phys. Rev. E* **56**, 6020 (1997).
  - [14] D. Y. Tang, W. S. Man, H. Y. Tam, and P. D. Drummond, *Phys. Rev. A* **64**, 033814 (2001).
  - [15] Ph. Grelu, F. Belhache, F. Guty, and J. M. Soto-Crespo, *Opt. Lett.* **27**, 966 (2002).
  - [16] A. Hideur, B. Ortaç, T. Chartier, M. Brunel, H. Leblond, and F. Sanchez, *Opt. Commun.* **225**, 71 (2003).
  - [17] Ph. Grelu and J. M. Soto-Crespo, *J. Opt. B: Quantum Semi-classical Opt.* **6**, S271 (2004).
  - [18] B. Ortaç, A. Hideur, T. Chartier, M. Brunel, Ph. Grelu, H. Leblond, and F. Sanchez, *IEEE Photon. Technol. Lett.* **16**, 1274 (2004).
  - [19] D. Y. Tang, L. M. Zhao, and B. Zhao, *Appl. Phys. B: Lasers Opt.* **80**, 239 (2005).
  - [20] Ph. Grelu, F. Belhache, F. Guty, and J. M. Soto-Crespo, *J. Opt. Soc. Am. B* **20**, 863 (2003).
  - [21] D. Y. Tang, B. Zhao, L. M. Zhao, and H. Y. Tam, *Phys. Rev. E* **72**, 016616 (2005).
  - [22] Ph. Grelu, J. Béal, and J. M. Soto-Crespo, *Opt. Express* **11**, 2238 (2003).
  - [23] A. Komarov and F. Sanchez, *Phys. Rev. E* **77**, 066201 (2008).
  - [24] A. Komarov, H. Leblond, and F. Sanchez, *Phys. Rev. E* **72**, 025604(R) (2005).
  - [25] A. Komarov, K. Komarov, H. Leblond, and F. Sanchez, *J. Opt. A, Pure Appl. Opt.* **9**, 1149 (2007).
  - [26] J. M. Soto-Crespo, N. Akhmediev, Ph. Grelu, and F. Belhache, *Opt. Lett.* **28**, 1757 (2003).
  - [27] N. Akhmediev, J. M. Soto-Crespo, M. Grapinet, and Ph. Grelu, *Opt. Fiber Technol.* **11**, 209 (2005).
  - [28] K. P. Komarov, *Opt. Spectrosc.* **60**, 231 (1986).
  - [29] N. N. Akhmediev and A. Ankiewicz, *Opt. Lett.* **19**, 545 (1994).
  - [30] C. Desem and P. L. Chu, *Optoelectron., IEE Proc. J.* **134**, 145 (1987).
  - [31] D. Y. Tang, B. Zhao, D. Y. Shen, C. Lu, W. S. Man, and H. Y. Tam, *Phys. Rev. A* **68**, 013816 (2003).
  - [32] D. Y. Tang, B. Zhao, D. Y. Shen, C. Lu, W. S. Man, and H. Y. Tam, *Phys. Rev. A* **66**, 033806 (2002).